

## SHORT COMMUNICATION

## Open Access

# Subcellular localization of $^{241}\text{Am}$ in structural components of submerged macrophyte of the River Yenisei *Elodea canadensis*

Lydia Bondareva<sup>1\*</sup>, Olga Mogilnaya<sup>2</sup> and Irina Vlasova<sup>3</sup>\* Correspondence: [lydiabondareva@gmail.com](mailto:lydiabondareva@gmail.com)<sup>1</sup>Siberian Federal University, Krasnoyarsk, Russia  
Full list of author information is available at the end of the article**Abstract**

We studied the microdistribution of the artificial radionuclide  $^{241}\text{Am}$  in the components of *Elodea canadensis* - a submerged macrophyte of the Yenisei River. The alpha-track analysis showed that the microdistribution of  $^{241}\text{Am}$  within different components of the submerged plant *E. canadensis* was not uniform.  $^{241}\text{Am}$  distribution was found to be affected by the age of the leaf blades, state of the cells, and morphological features of the plant stem. The radionuclide  $^{241}\text{Am}$  penetrated into the plant cells through the cell wall of *E. canadensis*, but it was accumulated in the vacuoles rather than in the cell wall or cytoplasm. In this case, the integrity of the cell membranes was not damaged.

**Keywords:** Submerged macrophyte, The Yenisei River, Subcellular localization, *Elodea canadensis*

**Findings**

The operation of nuclear fuel cycle facilities has led to the accumulation of artificial radionuclides in the environment. Whatever the pathway via which artificial radionuclides enter the environment (via aeolian transfer, with surface waters, with atmospheric precipitation), a considerable part of these radionuclides is transported to surface waters, where they interact with the components of the ecosystem. Thus, radionuclides are directly or indirectly involved in material cycling, getting redistributed among living organisms (including aquatic plants), sediments and floodplain soils, surface waters, and underflow groundwater. The most interesting ecosystem component for studying the accumulation, localization, and retention of radionuclides is aquatic plants (Abernethy et al. 1996; Barrat-Segretain 2001).

The aim of this study is to investigate the characteristics of the distribution and subcellular localization of the artificial radionuclide,  $^{241}\text{Am}$ , in the submerged macrophyte *Elodea canadensis*.

**Materials**

The experiments were performed on *E. canadensis* (Canadian waterweed) - a widely occurring submerged macrophyte species - collected from the Yenisei River. Young,

3-cm-long shoots were used; the total fresh biomass amounted to 6.5 g.  $^{241}\text{Am}$  in a 2-M  $\text{HNO}_3$  solution was twice added to the 200-mL experimental system.

### **Sample preparation**

Sample preparations were done for  $\alpha$ -track analysis, electron microscopy, and infrared (IR) spectroscopy.

#### ***Preparation of samples for $\alpha$ -track analysis***

Plants with the least damage, as assessed visually, leaves, and stems were selected for the analysis. They were separated into two parts: (1) the part of the plant that emerged in the course of the experiment (the juvenile part) and (2) the part of the plant that initially was 3 cm long (the senescent part). The plant parts were then spread flat and dried between glass slides.

#### ***Preparation of transversely cut stem sections for electron microscopy***

The plant stems taken out of the experimental system were cut into segments with the cross-sectional area up to 3 mm<sup>2</sup>. The segments were fixed, dehydrated, and embedded in an Epon 812 and Araldit M (Serva Electrophoresis GmbH, Heidelberg, Germany) resin mixture (1:1). When polymerization was completed, the samples were trimmed on a Reichert TM 60 (Reichert, Inc., Depew, NY, USA) block trimmer. The prepared longitudinally and transversely cut segments of biological tissues were trimmed using a Reichert UM-03 ultramicrotome glass knife (Puzyr' et al. 1998; Floriani 2005).

The plant segments were taken out of the water, and leaves and stems were cut into pieces up to 3 mm in size. The samples were fixed in 2.5% glutaric aldehyde in 0.1 M cacodylate buffer (pH 7.4) at 5°C for 3 h. After two washings with the buffer, they were again fixed in a 1% osmium tetroxide solution in the same buffer at 5°C for 1.5 to 2 h. The samples were washed to remove the fixative with the buffer (twice for 5 min each) and dehydrated in a series of increasing ethanol concentrations and in acetone according to the following scheme: 50% ethanol, two times for 5 min; 70% ethanol, two times for 10 min; 96% ethanol, two times for 15 min; 100% ethanol, three times for 20 min; and acetone, three times for 20 min. Dehydration and further impregnation procedure of the samples with epoxy resin were carried out at room temperature. The mixture of the epoxy resins Epon 812 and Araldit M (1:1; Serva) was then used. Polymerization was performed for 12 h at 48°C and for 48 h at 60°C. Ultrathin sections were obtained using an ultramicrotome Reichert UM-03 and examined using an electron microscope JEM 1400 (JEOL Ltd., Akishima, Tokyo, Japan). When preparing the samples for the examination, the sections were not additionally contrasted with heavy metal salts (namely, lead isocitrate).

#### ***Preparation of samples for IR spectroscopy***

The samples of air-dry plant mass were finely crushed. The obtained crushed sample was then mixed with KBr, which was used as a matrix, and molded into tablets. All the samples were prepared under the same conditions (time of mixing with potassium bromide, molding pressure, vacuumization time). The same concentration of the dry plant mass was used - 6 mg dry plant mass/1,000 mg KBr.

## Methods

### *Liquid scintillation spectrometry*

$^{241}\text{Am}$  concentration in the water and other liquids was measured using liquid scintillation spectrometry on a Tri-Carb-2800 spectrometer (Canberra Industries Co., Meriden, CT, USA). Immediately before the measurement, an aliquot of the liquid was mixed with an Ultima Gold AB scintillation cocktail (PerkinElmer, Waltham, MA, USA) at a ratio of 8:12 (sample/cocktail) in a plastic vial. The volume of the measured samples was 20 mL. Each measurement lasted 300 to 420 min.

### *Gamma spectrometry*

$^{241}\text{Am}$  concentration in the liquid and solid samples was measured on a  $\gamma$ -spectrometer (Canberra, USA) coupled to an HPGe hyper-pure germanium detector, capable of measuring  $\gamma$ -spectra in the energy range from 30 to 3,000 keV. The  $\gamma$ -spectra were processed using the Canberra Genie PC software (Canberra, USA).

### *$\alpha$ -Track analysis*

The prepared flat biological samples were covered with fragments of CR-39 polycarbonate  $\alpha$ -track detector and were left tightly pressed for a certain time period, which varied between 87 and 1,130 h, depending on the  $^{241}\text{Am}$  concentration. Fragments of the  $\alpha$ -track detector were then separated from the plant samples and placed into a 7.25-M NaOH solution, where they were left to stay for 6 h at 70°C. The  $\alpha$ -particle tracks thus detected were analyzed using an Ergaval Carl Zeiss optical microscope (Carl Zeiss AG, Oberkochen, Germany) at magnifications of  $\times 32$ ,  $\times 100$ , and  $\times 160$ . Micrographs of fragments of the  $\alpha$ -track detector were made using a Canon Power Shot SD100 digital camera (Canon USA, Inc., Lake Success, NY, USA).

### *Fourier transform infrared spectrometry*

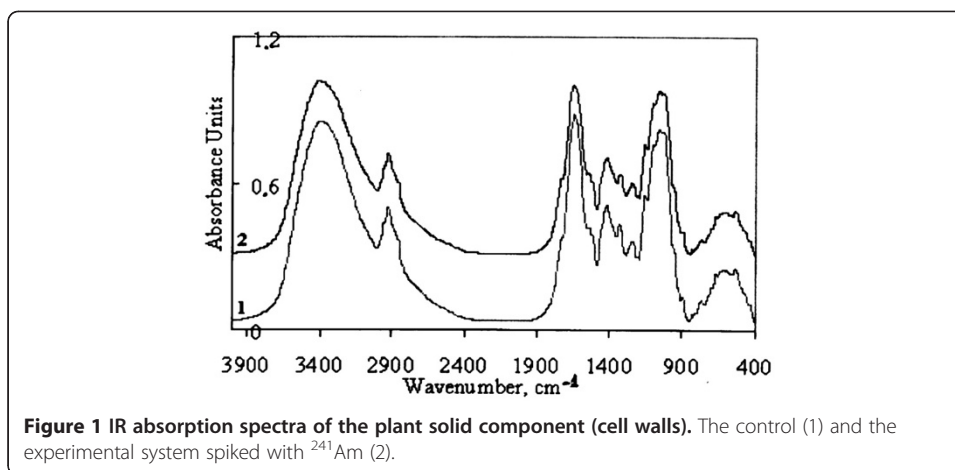
Spectra in the range 4,000 to 400  $\text{cm}^{-1}$  were registered using a Bruker FT-IR spectrometer (model Tensor 27, BRUKER OPTIK GMBH, Ettlingen, Germany); reflectance spectra were registered using an EasiDiff diffuse reflectance accessory (BRUKER, Germany). The spectral data were processed using the OPUS 5.0 software (Medical Software Systems, Tucson, AZ, USA).

## Results and discussion

### *Accumulation and distribution of $^{241}\text{Am}$ in *E. canadensis* samples*

The total amount of  $^{241}\text{Am}$  added to the system was  $1850 \pm 31$  Bq/L, or  $370 \pm 6$  Bq in 200 mL. The radionuclide was added twice. Its primary added activity was  $750 \pm 7$  Bq/L. After 120 h, when a significant activity decrease was registered (up to  $120 \pm 7$  Bq/L), more  $^{241}\text{Am}$  was added. After the second addition of  $^{241}\text{Am}$ , its total activity was 1,210 Bq/L or approximately 240 Bq per sample. After 216 h of the experiment,  $^{241}\text{Am}$  activity in the water dropped to  $388 \pm 4$  Bq/L (78 Bq). The total amount of  $^{241}\text{Am}$  accumulated by the plants was 182 Bq per sample, or 758,333 Bq/kg dry mass. After the biomass had been separated into the solid cell parts (cell walls, membranes, intracellular organelles, etc.) and the intracellular fluid, those components were also measured to determine  $^{241}\text{Am}$  activity. About 85% of accumulated  $^{241}\text{Am}$  was found in the structural (solid) parts of the cells.

Figure 1 shows IR absorption spectra of the plant solid components (cell walls, membranes, intracellular organelles, etc.) of the control (without  $^{241}\text{Am}$  addition) and of the



experimental system. These spectra contain intense absorption bands with peaks at about  $3,400$  and  $1,656\text{ cm}^{-1}$ . An intense broad absorption band within the spectral region  $3,700$  to  $2,200\text{ cm}^{-1}$  (with the major peak at about  $3,400\text{ cm}^{-1}$ ) is ascribed to stretching vibrations of hydrogen-bonded hydroxyl groups, and the absorption band at  $1,656$  and  $620\text{ cm}^{-1}$  is due to deformation vibrations of the OH groups (Coates 2000; Nakamoto 2009). The absorption bands in the regions  $3,000$  to  $2,800$  and  $1,450$  to  $1,370\text{ cm}^{-1}$ , respectively, refer to stretching and deformation vibrations of the aliphatic  $\text{CH}_3-$  and  $\text{CH}_2-$  groups (Coates 2000; Nakamoto 2009). The absorption band with the peak at  $1,735\text{ cm}^{-1}$  is ascribed to stretching vibrations of the carbonyl groups. Moreover, the analysis of the absorption bands in the spectral region  $1,000$  to  $1,200\text{ cm}^{-1}$  in combination with the absorption at  $1,735\text{ cm}^{-1}$  suggests the presence of keto ester compounds in the structural components of the cell (Coates 2000).

The analysis of the curves in Figure 1 suggests that the samples were spectrally almost identical to each other. Similar results were also obtained for the diffuse reflectance spectra. Thus, although the major portion of  $^{241}\text{Am}$  was bound with solid cell components, the chemical structure of cell walls, membranes, and intracellular organelles of  $^{241}\text{Am}$ -treated plants remained unaffected by the radionuclide.

#### $^{241}\text{Am}$ microdistribution

The density of  $\alpha$ -particle tracks (the number of tracks per millimeter square) for different structural parts of the plant samples was determined using crosshairs. These crosshairs were used to measure the area of a leaf or stem section on which the number of tracks was calculated. The calculation of the specific activity of a sample segment is just an estimate because the distance between the sample and the detector is indeterminate as is the contribution of  $\alpha$ -particle tracks on the leaf underside. For the spread flat dried plant samples, the track registration coefficient of 0.74 was used. The registration coefficient for the stem segments embedded in the epoxy resins and trimmed ones was 0.9, which was a characteristic of smoothly trimmed sections adhering to the detector (Ilic and Durrani 2003; Omel'yanenko et al. 2007). As the samples analyzed using the  $\alpha$ -track detector were all exposed to the same conditions, activities in different structural parts of the sample can be compared, neglecting the registration coefficient.

The  $\alpha$ -track analysis of *E. canadensis* samples kept in  $^{241}\text{Am}$ -spiked solution showed the following: the microdistribution of  $^{241}\text{Am}$  both on the plant surface and inside the

plant was nonuniform. In our earlier research, at least three reasons were found to determine the  $^{241}\text{Am}$  distribution (Figure 2):

1. Shoot age is based on the analysis of the whole plant: between the juvenile and the senescent parts of the shoot (Figure 2a).
2. State of the cells, living and dead, is based on the analysis of the leaf blade surface: between the main part of the leaf blade (green-colored cells) and the dead parts of the leaf epidermis (brown-colored cells) (Figure 2b,c).
3. Morphological features of the plant stem are based on the analysis of the transversely cut stem segment: between the external surface of the stem and its inner part (Figure 3). The distribution of americium in the plant was thoroughly examined.

#### **Subcellular localization of $^{241}\text{Am}$**

Americium is a heavy metal; thus, its accumulations in the ultrathin sections would appear as electron-dense areas. The analysis of the ultrathin sections of *E. canadensis*

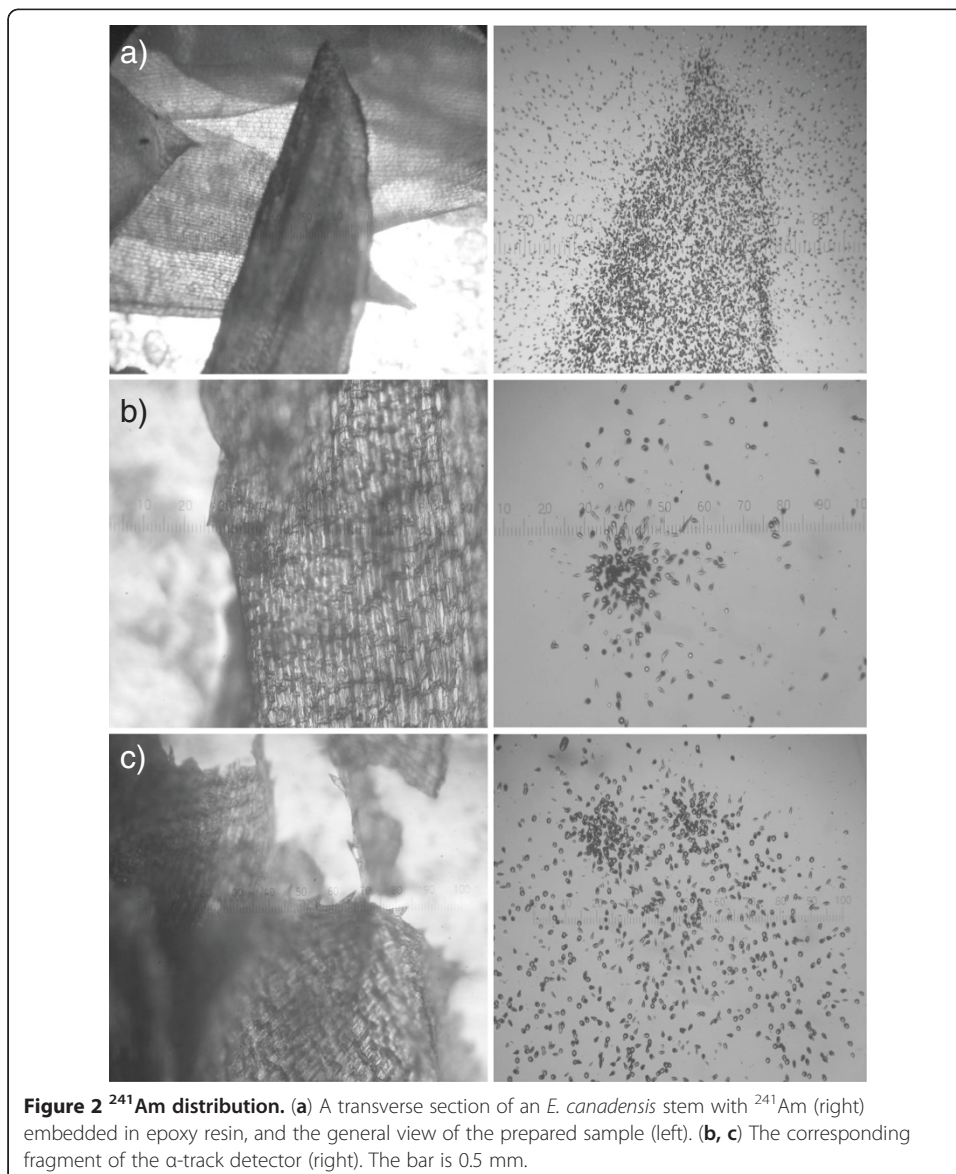


**Figure 2**  $^{241}\text{Am}$  distribution. (a) A transverse section of an *E. canadensis* stem with  $^{241}\text{Am}$  (right) embedded in epoxy resin, and the general view of the prepared sample (left). (b, c) The corresponding fragment of the  $\alpha$ -track detector (right). The bar is 0.5 mm.

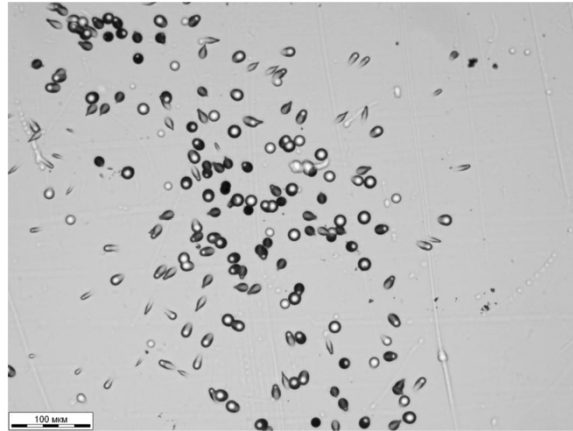


**Figure 3** A transverse section of an *E. canadensis* stem with  $^{241}\text{Am}$ . It is embedded in epoxy resin. It shows the evaluation of the  $^{241}\text{Am}$ -containing layer. The bar is 100  $\mu\text{m}$ .

leaves and stems revealed that the accumulations of the heavy metal particles were observed in the vacuoles (Figure 4). Moreover, the vacuole envelope (tonoplast) was strongly contrasted in the sections, indicating the presence of the heavy metal. It is known that vacuoles and tonoplast play an essential role in cellular homeostasis, nutrition, and growth of plant cells. Substances arrive in the vacuoles from the cytoplasm by protein transporters and through channels in the tonoplast (Reisen et al. 2005). Therefore, radionuclide accumulations were fixed in these parts of the cell.

When examining the ultrathin sections, no radionuclide accumulation was found in the cell wall or any other cell organelles or cytoplasm.

With the increase of the intensity and ratio of the impact of the  $^{241}\text{Am}$  solution in the plant cells, the increased content of the electron-dense accumulations in the vacuoles was observed (Figure 5), confirming that the electron-dense conglomerates were americium salts.

It is worth noting that during the life activity of a plant, oxalic acid is often released into the vacuole; its salts (calcium oxalates) are sometimes deposited as single crystals

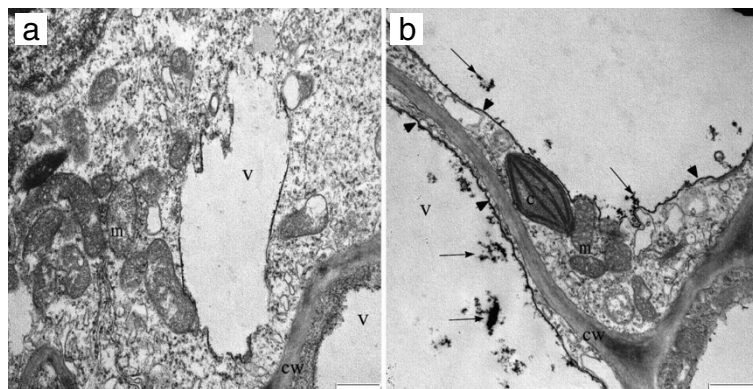


**Figure 4** Ultrathin stem sections of *E. canadensis*. (a) Intact plant (control), (b) plant incubated with the radionuclide (v, vacuole; c, chloroplast; cw, cell wall; m, mitochondrion; the arrows show the electron-dense accumulations in the vacuoles). The bar is 1  $\mu\text{m}$ .

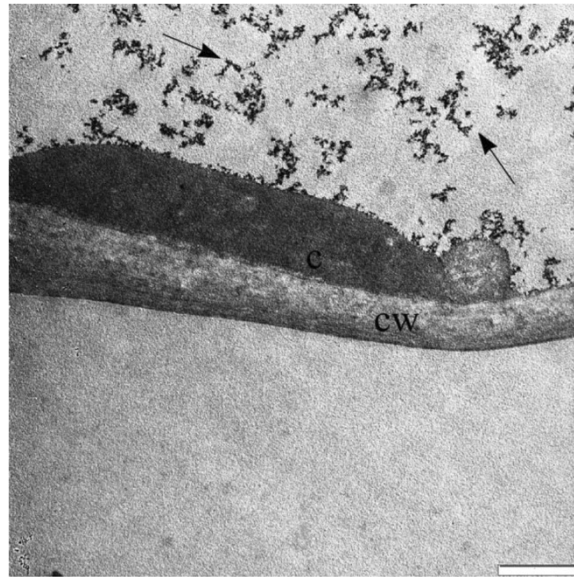


**Figure 5** Accumulations of americium salts in the cell vacuole at increased level of the radionuclide impact. c, Chloroplast; cw, cell wall. The bar is 1  $\mu\text{m}$ .

or as needlelike conglomerates of the crystals of this salt - raphides. However, their electron density is always lower than that of the americium accumulations (Figure 6).

### Conclusions

The  $\alpha$ -track analysis showed that the microdistribution of  $^{241}\text{Am}$  within different components of the submerged plant *E. canadensis* was not uniform.  $^{241}\text{Am}$  distribution was found to be affected by (1) the age of the leaf blades, (2) the state of the cells, and (3) morphological features of the plant stem. The radionuclide  $^{241}\text{Am}$  penetrated into the plant cells through the cell wall of *E. canadensis* but was accumulated in the vacuoles rather than in the cell wall or cytoplasm.

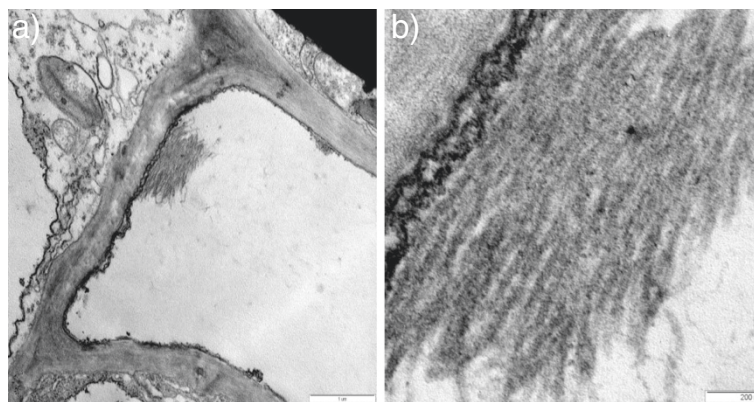


**Figure 6** Calcium oxalate crystals (arrow) in the cell vacuole of *E. canadensis*. The bar is (a) 1  $\mu\text{m}$  and (b) 200 nm.

#### Competing interests

The authors declare that they have no competing interests.

#### Authors' contributions

LB is the mastermind behind the submitted work, conducted experiments on the accumulation of radionuclide, *Elodea canadensis*, and certain radionuclides using liquid scintillation spectrometry. Her primary role was to write this article. OM conducted microscopic studies in subcellular studies and wrote a chapter on the subcellular distribution of the radionuclide in the plant. IV did the  $\alpha$ -track analysis of the samples with the accumulation of radionuclides and participated in the discussion of the general concept of work and publication. All authors read and approved the final manuscript.

#### Acknowledgments

The work was partly supported by the State Contract Ministry of Education and Science N 16.512.11.2131 (25.02.2011).

#### Author details

<sup>1</sup>Siberian Federal University, Krasnoyarsk, Russia. <sup>2</sup>Institute of Biophysics SB RAS, Krasnoyarsk, Russia. <sup>3</sup>Moscow State University, Moscow, Russia.

Received: 25 March 2012 Accepted: 14 August 2012

Published: 24 August 2012

#### References

- Abernethy VJ, Sabbatini MR, Murphy KJ (1996) Response of *Elodea canadensis* Michx. and *Myriophyllum spicatum* L. to shade, cutting and competition in experimental culture. *Hydrobiologia* 340:219–224
- Barrat-Segretain H (2001) Invasive species in the Rhone River floodplain (France): replacement of *Elodea canadensis* Michaux by *Elodea nuttallii* St. John in two former river channels *Arch Hydrobiologia* 152:237–251
- Coates J (2000) Interpretation of infrared spectra, a practical approach. In: Meyers RA (ed) *Encyclopedia of analytical chemistry*. John Wiley & Sons Ltd, Chichester, pp 10815–10837
- Floriani M (2005) Subcellular localization of radionuclides by transmission electronic microscopy: Application to uranium, selenium and aquatic organisms. *Radioprotection* 40(suppl 1):S211–S216
- Ilic R, Durrani SA (2003) Solid state nuclear track detectors, In: *Handbook of radioactivity analysis*. Elsevier Science, USA, p 685
- Nakamoto K (2009) Infrared and Raman spectra of inorganic and coordination compounds. Part A: theory and applications in inorganic chemistry, 6th edn. Wiley, New York, p 432
- Omelyanenko B, Petrov V, Poluektov V (2007) Behavior of uranium under conditions of interaction of rocks and ores with subsurface water. *Geology of Ore Deposits* 49(5):378–391
- Puzyr' AP, Mogil'naya OA, Tirranen LS (1998) Architectonics of *Flavobacterium* sp. 56 and *Flavobacterium* sp. 22 colonies as exposed by transmission electron microscopy. *Microbiologiya (Microbiology)*. 67., pp 672–679, in Russian
- Reisen D, Marty F, Leborgne-Castel N (2005) New insights into the tonoplast architecture of plant vacuoles and vacuolar dynamics during osmotic stress. *BMC Plant Biol* 5:13

doi:10.1186/2008-6970-4-13

**Cite this article as:** Bondareva et al.: Subcellular localization of <sup>241</sup>Am in structural components of submerged macrophyte of the River Yenisei *Elodea canadensis*. *International Aquatic Research* 2012 **4**:13.

Submit your manuscript to a SpringerOpen<sup>®</sup> journal and benefit from:

- Convenient online submission
- Rigorous peer review
- Immediate publication on acceptance
- Open access: articles freely available online
- High visibility within the field
- Retaining the copyright to your article

Submit your next manuscript at ► [springeropen.com](http://springeropen.com)